

## Voxel-wise analysis of 18F-fluorodeoxyglucose metabolism in correlation with variations in the presentation of Alzheimer's disease: a clinician's guide

Siti Aishah Abdul Aziz,<sup>1,2</sup> Loh Jia Ling,<sup>1</sup> Fathinul Fikri Ahmad Saad,<sup>1</sup> Abdul Jalil Nordin,<sup>1</sup> Normala Ibrahim,<sup>3</sup> Arlina Nuruddin,<sup>4</sup> Elinda Tunan,<sup>5</sup> Rosalina,<sup>6</sup> M. Iqbal Saripan,<sup>7</sup> Subapriya Suppiah<sup>1,3</sup>

pISSN: 0853-1773 • eISSN: 2252-8083  
<https://doi.org/10.13181/mji.v28i3.2770>  
**Med J Indones.** 2019;28:300–8

**Received:** May 05, 2018

**Accepted:** July 19, 2019

### Authors' affiliations:

<sup>1</sup>Centre for Diagnostic Nuclear Imaging, Universiti Putra Malaysia, Selangor, Malaysia, <sup>2</sup>School of Health Sciences, Universiti Sains Malaysia, Kelantan, Malaysia, <sup>3</sup>Faculty of Medicine and Health Sciences, Universiti Putra Malaysia, Selangor, Malaysia, <sup>4</sup>Department of Psychiatry and Mental Health, Kajang Hospital, Selangor, Malaysia, <sup>5</sup>Department of Psychiatry, Serdang Hospital, Selangor, Malaysia, <sup>6</sup>Dharmais Cancer Hospital, Jakarta, Indonesia, <sup>7</sup>Department of Computer and Communication Systems Engineering, Faculty of Engineering, Universiti Putra Malaysia, Selangor, Malaysia

### Corresponding author:

Subapriya Suppiah  
 Centre for Diagnostic Nuclear Imaging,  
 Universiti Putra Malaysia, 43400  
 Serdang, Selangor, Malaysia  
 Tel/Fax: +60-389471641/+60-389472775  
 E-mail: [subapriya@upm.edu.my](mailto:subapriya@upm.edu.my)

### ABSTRACT

**BACKGROUND** Diagnostic imaging can be applied in the management of Alzheimer's disease as it provides structural and functional information to exclude possible secondary causes and offers additional information, especially in atypical cases of Alzheimer's disease. The utility of positron emission tomography/computed tomography (PET/CT) can help in the noninvasive diagnosis of Alzheimer's disease by voxel-wise quantification of cerebral 18F-fluorodeoxyglucose (FDG) metabolism.

**METHODS** This prospective study was conducted among 10 subjects with Alzheimer's disease and 10 healthy control subjects who underwent neuropsychological testing and 18F-FDG PET/CT scans. Images of the brain were postprocessed using voxel-wise analysis and segmented into 20 regions of interest. The standardized uptake value  $(SUV)_{max}/SUV_{mean}$ /standard deviation of  $SUV_{mean}$  results were analyzed accordingly and correlated with the subjects' Montreal cognitive assessment (MoCA) results that were adjusted for age and education level.

**RESULTS** Hypometabolism at the right parietal lobe significantly correlated with increasing age and lower MoCA scores. Global hypometabolism was observed in subjects who had advanced Alzheimer's disease but preserved primary somatosensory cortices (S1) region metabolism. Predominance of frontal lobe hypometabolism was a feature of subjects with Alzheimer's disease having associated depressive symptoms.

**CONCLUSIONS** 18F-FDG PET/CT voxel-wise analysis can be used for quantitative assessment and can assist clinicians in the diagnosis of Alzheimer's disease and other variations of the disease spectrum.

**KEYWORDS** dementia, geriatrics, molecular imaging, neurocognitive disorder, neurology, positron emission tomography

Alzheimer's disease is classified as a major neurocognitive disorder (NCD) based on the Diagnostic and Statistical Manual of Mental Disorders, Fifth Edition (DSM-5).<sup>1</sup> Its incidence has been increasing and represents the commonest type of NCDs, contributing to 65% of all patients with NCD, followed by vascular-type NCD (vascular dementia/VaD) (20%) and Lewy body-type NCD (10–15%).<sup>2</sup> Clinically, patients with NCD present with a progressive decline in various intellectual domains, including memory, language, and executive function.<sup>1</sup> Neuropsychological assessments using screening tools such as the Mini-Mental State Examination

have been criticized for their lack of sensitivity and their dependency on age and level of education.<sup>3</sup> In contrast, the Montreal cognitive assessment (MoCA) has been reported to have a higher sensitivity (100%), a higher reliability, and a better internal consistency for detecting NCDs and mild neurocognitive impairments.<sup>4</sup> However, till date, there are no established clinical diagnostic criteria that can be applied to accurately diagnose this disease, which has consequently resulted in a large majority of people with Alzheimer's disease being underdiagnosed. Hence, these people are unable to gain access to proper care and treatment.<sup>5</sup>

Copyright © 2019 Authors. This is an open access article distributed under the terms of the Creative Commons Attribution-NonCommercial 4.0 International License (<http://creativecommons.org/licenses/by-nc/4.0/>), which permits unrestricted non-commercial use, distribution, and reproduction in any medium, provided the original author and source are properly cited.

The National Institute on Aging-Alzheimer's Association has proposed the following three biomarkers in the clinical diagnosis of Alzheimer's disease: (i) medial temporal lobe atrophy assessed by structural imaging, (ii) evidence of hypometabolism at the temporoparietal lobes assessed using 18F-fluorodeoxyglucose positron emission tomography (18F-FDG PET), and (iii) elevated amyloid binding on amyloid PET.<sup>6</sup> Unfortunately, a definitive diagnosis can be made only at autopsy when specific pathological lesions, including the intracellular neurofibrillary tangles, amyloid- $\beta$  plaques, synapse/neuronal loss, and atrophy, are observed.<sup>7</sup> Diagnostic imaging can play a role in the management of NCDs by providing structural and functional information to exclude possible secondary causes and offering additional information to differentiate the subtypes, especially in atypical cases. The use of functional imaging in clinical practice, such as technetium-99m-hexamethylpropylene amine oxime SPECT and 18F-FDG positron emission tomography/computed tomography (PET/CT), as well as amyloid imaging PET/CT, is gaining momentum as noninvasive imaging biomarkers to provide a better diagnostic accuracy.<sup>8-10</sup>

Molecular imaging using 18F-FDG PET/CT has been widely used for oncology imaging,<sup>8,11</sup> and also for diagnosing infection,<sup>12</sup> neurology, and cardiology cases.<sup>13</sup> Previous research has shown that 18F-FDG PET/CT can act as a noninvasive biomarker of cognitive decline and this imaging technique is widely available in several centers.<sup>14</sup> Measurement of cerebral glucose hypometabolism acts as a surrogate biomarker for NCDs, wherein reduced activity in the temporoparietal lobes of the brain is a hallmark of Alzheimer's disease.<sup>15</sup> The quantitative measurement for PET/CT uses standardized uptake values (SUVs) that take into account the ratio of FDG distribution in the body.<sup>16</sup> The literature reports studies that have analyzed voxel-wise regional 18F-FDG hypometabolism as evidenced by reduced SUVs to help in the objective assessment of patients with NCD.<sup>17</sup> The commonly cited areas of hypometabolism are the medial, temporal, and hippocampal regions.<sup>18</sup> Furthermore, the entorhinal cortex has an advantage over the hippocampus in early Alzheimer's disease and in predicting the progression of subjects with mild cognitive impairment to Alzheimer's disease.<sup>19</sup> It has also been observed that 18F-FDG hypometabolism occurs in the precuneus, posterior

cingulate, parietal, and temporal cortices, even before the onset of symptoms of Alzheimer's disease, which subsequently extends into the frontal cortex and the entire brain in advanced stages of Alzheimer's disease.<sup>20</sup> To further complicate matters, a heterogeneous distribution of 18F-FDG has been reported even in healthy elderly subjects and an atypical distribution of hypometabolism in subjects with Alzheimer's disease, which can confound the clinicians when diagnosing Alzheimer's disease.<sup>21</sup>

Therefore, it is proposed for a voxel-wise quantitative assessment of cortical 18F-FDG distribution in patients with Alzheimer's disease to explore variations in glucose metabolism. The aim of this study was to correlate 18F-FDG PET/CT imaging biomarkers with clinical findings that can act as a guide to clinicians dealing with atypical cases of Alzheimer's disease. The pattern of 18F-FDG distribution in noncognitive behavioral changes in subjects with Alzheimer's disease was also explored.

## METHODS

### Study participants

A prospective case-control study was conducted after receiving ethical clearance from the institutional ethical committee (No. PPDN(FR14)P032). Subjects aged 55-80 years with a diagnosis of Alzheimer's disease were recruited from the memory clinics in two centrally located regional hospitals in Kuala Lumpur, Malaysia, according to the criteria set by the Declaration of Helsinki. A total of 18 subjects with Alzheimer's disease were recruited and scanned in 2018; however, 8 subjects withdrew from the study due to anxiety regarding the examination. Healthy subjects within the stipulated age group (control population) were also recruited from the general population in Kuala Lumpur who responded to advertisements by the research team. The subjects provided written informed consent to participate in this study. The inclusion criteria were patients with a normal serum creatinine level and being cooperative for the PET/CT examination, whereas the exclusion criteria were patients with uncontrolled blood sugar levels and psychotic subjects.

### Neuropsychological assessment

Subjects with Alzheimer's disease and healthy volunteers were assessed by a conventional neuropsychological screening tool using the MoCA

test. A cut-off point of 26 is generally used to classify patients with Alzheimer's disease (<26 points) in contrast to healthy controls having higher scores (≥26 points).<sup>4</sup> Furthermore, the corrected the MoCA scores for age group and education level of the subjects to classify them as having Alzheimer's disease, was based on the study of Borland et al.<sup>22</sup>

### Imaging protocol

A total of 20 participants (10 subjects with Alzheimer's disease and 10 healthy controls) underwent 18F-FDG PET/CT imaging. The subjects were given intravenous 18F-FDG of approximately 5 mCi and kept rested in a dark room. After an uptake period of approximately 60 min, the subjects underwent a CT scan of the brain from the skull base to the vertex, followed by a contemporaneous PET/CT imaging. The scans were performed on a 64-slice multidetected hybrid PET/CT scanner (Siemens Truepoint Biograph TrueV®) equipped with a lutetium oxyorthosilicate scintillator crystal camera. The 64-slice CT scanner was used to image the brain, and the imaging was performed at 120 kVp, 110 mAs, 0.8 pitch, and 1.0 s per gantry rotation time; detector configuration of 64 × 0.625 mm; and 3.0-mm slice thickness. Image reconstruction was performed using filtered back projection with a Gaussian smoothing of 2-mm full width at half-maximum.

### Image interpretation

The CT scan images were viewed on a high-resolution image processing workstation (Syngo.via Multi-Modality Workstation). Visual assessment was performed to detect any morphological abnormalities in the cross-sectional CT scan images. Then, using the image cortical radioisotope uptake processing software (Syngo.via MI Neurology), a 3D voxel-wise assessment software, the attenuation-corrected CT scan images were aligned and fused to the PET images. Subsequently, the images were fused to the normal template atlas. The FDG-PET biography (SMART Neuro AC) template that was composed of the data of healthy subjects aged 46–79 years comprising both genders were selected. Subsequently, voxel-wise assessment of 18F-FDG metabolism was done based on the following formula:

$$\text{Statistic} = \frac{(\text{Patient value} - \text{Population mean})}{\text{Population standard deviation}}$$

An anatomical review was conducted by scrutinizing the uptake of 18F-FDG in several regions of interest (ROIs), namely, the hippocampus; the frontal, temporal, parietal, and occipital lobes; and the primary somatosensory cortex (S1). The mean SUV ( $SUV_{\text{mean}}$ ) and the standard deviations (SD) from the mean were evaluated. The images and the quantitative parameters were assessed by two consultant radiologists with nuclear medicine training by consensus and were compared with the clinical findings. Voxels that demonstrated SUVs that were two SD below the normal template were considered to have significant hypometabolism. These areas were assessed regionally and depicted in dark blue color coding. In contrast, areas that had more than two SD of  $SUV_{\text{mean}}$  from the normal template were considered to have hypermetabolism and depicted in red color coding.

### Statistical analysis

ROIs as tabulated by the software were assessed, and the SUVs together with the SD values were extracted and tabulated. General demographic data of the patient characteristics were described using tables for categorical data, and median values and range were used for representing continuous variables. The SPSS software, version 25 (IBM), was used for all statistical analyses. Voxel-by-voxel assessment for individual subjects and cross-group correlations were conducted. For ROI-wise correlation analysis, the statistical significance was defined as  $p < 0.05$  (2-tailed). Independent variables of age, gender, race, and MoCA results, as well as the duration of diagnosis, were correlated with the imaging parameters using Pearson's correlation for age, duration of diagnosis, and MoCA results; student t-test was used for evaluating gender and diagnosis, and one-way analysis of variance was used for race. Subsequent analyses of the association of age, gender, race, and MoCA results were performed after classifying the subjects into the Alzheimer's disease group and the healthy group using t-test.

## RESULTS

### Population demographics

The 10 subjects with Alzheimer's disease comprised 9 women and 1 man (aged 62–80 years, mean (SD) = 74.9 [6.5]). The healthy controls consisted of 7 women

**Table 1.** Comparison of variables between the two groups of patients

Variables	Healthy group min–max; mean (SD)	Alzheimer’s disease group min–max; mean (SD)	<i>p</i>
Age (years)	61–70; (65.4 [2.9])	62–80; (74.9 [6.5])	<b>0.003*</b>
Duration of symptoms (years)	-	1.0–5.0; (2.9 [1.5])	0.508 <sup>†</sup>
MoCA scores (points)	26–28; (27.4 [0.70])	0–20; (10.6 [5.6])	<b>&lt;0.001*</b>
SUV <sub>max</sub> (g/ml), min–max			
Right temporal	17.1–29.9	18.4–26.0	0.916
Left temporal	16.2–27.9	19.3–26.4	0.803
Right parietal	18.2–31.2	19.4–27.7	0.926
Left parietal	18.0–30.6	19.3–27.2	0.918
SD of SUV <sub>mean</sub> (g/ml), mean (SD)			
Right parietal	-0.54 (1.4)	-5.6 (9.0)	<b>0.043*</b>
Left parietal	-0.79 (1.5)	-6.0 (9.2)	<b>0.039*</b>
Left cingulate gyri	-1.5 (1.7)	-4.0 (2.6)	<b>0.021*</b>
Right cingulate gyri	-1.2 (1.5)	-3.7 (3.2)	<b>0.036*</b>

SD=standard deviation; MoCA=Montreal cognitive assessment; SUV=standardized uptake value

\*using independent sample t-test; <sup>†</sup>using Pearson’s correlation

and 3 men. Demographic data of the subjects are depicted in Table 1. The mean MoCA scores were also corrected for age and education level.

#### Quantitative 18F-FDG PET/CT parameters

The maximum SUV (SUV<sub>max</sub>) and SUV<sub>mean</sub>, as well as the SD of the mean, of the ROIs in the cortices of the brain were calculated. The ROIs were primarily focused on bilateral frontal, temporal, parietal, and occipital lobes and cingulate and paracingulate gyri, central lobes, calcarine fissure, basal ganglia, mesial temporal lobes, and the cerebellum.

Pearson’s correlation revealed an inverse relationship between the SD of the SUV<sub>mean</sub> of selected brain lobes and age, i.e., 18F-FDG hypometabolism in the selected regions of the brain significantly correlated with increasing age (Table 2). In particular, the right parietal lobes and the bilateral cingulate and paracingulate gyri significantly correlated between the two groups of subjects as well as in terms of increasing age.

The Pearson’s correlation also demonstrated a strong relationship between MoCA scores and the SD of SUV<sub>mean</sub> values. Strong positive correlations were

**Table 2.** Correlation between SUV<sub>mean</sub> and age, MoCA scores in each brain region

Brain regions	Correlation SUV <sub>mean</sub> & age		Correlation SUV <sub>mean</sub> & MoCA scores	
	<i>r</i>	<i>p</i> *	<i>r</i>	<i>p</i> *
Right temporal	-0.463	0.04	0.548	0.012
Left temporal	-	-	0.520	0.019
Right parietal	-0.533	0.015	0.669	0.001
Left parietal	-	-	0.703	0.001
Right frontal	-0.517	0.019	0.644	0.002
Left frontal	-0.470	0.037	0.645	0.002
Right cingulate and paracingulate gyri	-0.533	0.016	-	-
Left cingulate and paracingulate gyri	-0.0542	0.014	0.444	0.05
Left occipital	-	-	0.486	0.03
Left basal ganglia	-	-	0.449	0.047

SUV=standardized uptake value; MoCA=Montreal cognitive assessment

\*Significant at the *p* < 0.05 (2-tailed)

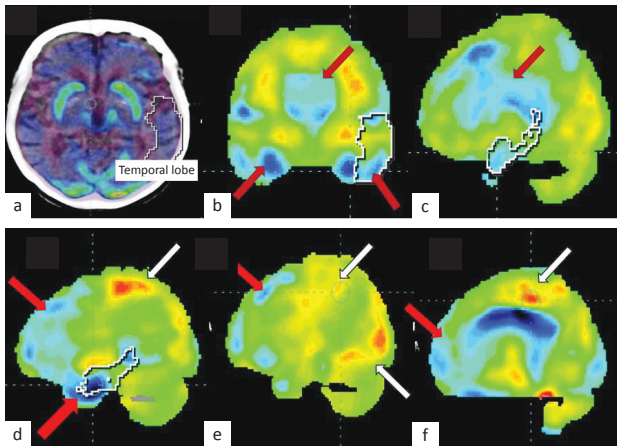


**Figure 1.** PET/CT brain images in: (a) axial; (b) coronal; (c) sagittal of subjects with typical Alzheimer's disease demonstrating  $^{18}\text{F}$ -FDG hypometabolism at the medial temporal lobes (red arrows); (d, e, f) coronal views of  $^{18}\text{F}$ -FDG PET/CT scans of a patient with advanced Alzheimer's disease demonstrating hypometabolism (red arrows) at the posterior cingulate, temporal lobes, and the prefrontal cortex with preserved metabolism (white arrows) at S1 and the visual cortex.  $^{18}\text{F}$ -FDG PET/CT= $^{18}\text{F}$ -fluorodeoxyglucose positron emission tomography/computed tomography

observed between MoCA scores and the  $\text{SUV}_{\text{mean}}$  in almost all the lobes of the brain (Table 2). However, there were no significant associations between the duration of diagnosis of patients with Alzheimer's disease and the SUVs of the brain lobes.

### Correlation between $^{18}\text{F}$ -FDG PET/CT metabolism patterns and clinical findings

Subjects with a typical presentation of Alzheimer's disease had progressive memory loss that had implications on the basal isocortical regions. As shown in Figure 1 (a, b, c), the dark blue regions (red arrows) indicate  $^{18}\text{F}$ -FDG hypometabolism in the medial temporal lobes and parietal lobes. Global hypometabolism was detected in cases of advanced Alzheimer's disease, wherein generalized, bilateral regions of hypometabolism were observed. The generalized dark blue regions (red arrows) depicted in Figure 1 (d, e, f) demonstrate reduced  $^{18}\text{F}$ -FDG metabolism indicative of widespread cortical dysfunction. Interestingly, there were preserved metabolism and, in certain instances, hypermetabolism at the S1 as indicated by the white arrows.

Alzheimer's disease can exist concurrently with VaD. VaD alone can be very subtle in its onset and masked by patterns of stroke symptoms. However, fluctuating memory loss corresponding

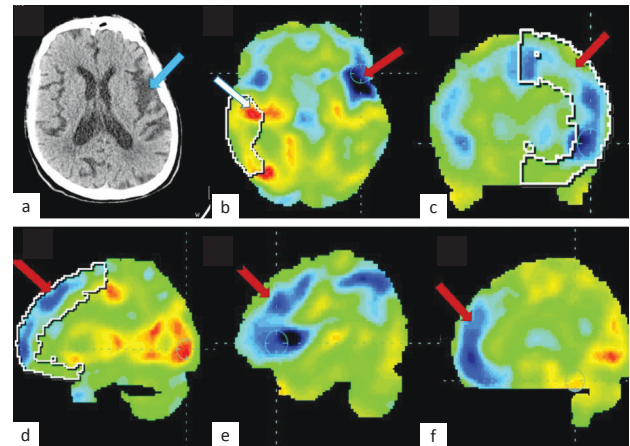


**Figure 2.** A subject with a history of left temporal stroke and progressive memory loss. (a) CT brain image in the axial view demonstrating hypodensity at the left temporal region consistent with a left middle cerebral artery territory and watershed area infarct (blue arrow); (b) the corresponding  $^{18}\text{F}$ -FDG hypometabolism in the axial view at the left temporal lobe and watershed areas (red arrow). The white arrow in Figure 3b indicates an area of glucose hypermetabolism at the contralateral lobe probably due to a compensatory effect caused by shunting of blood; (c) depicts  $^{18}\text{F}$ -FDG PET/CT scan in the coronal view showing hypometabolism in the temporoparietal regions (red arrow); (d, e, f) A subject diagnosed with Alzheimer's disease and having concurrent behavioral changes. All the coronal-view  $^{18}\text{F}$ -FDG PET/CT images demonstrate typical hypometabolism in the temporal lobes with an additional predominance in the prefrontal cortex and frontal lobe (red arrows), indicative of the metabolism changes caused by a concurrent mood disorder.  $^{18}\text{F}$ -FDG PET/CT= $^{18}\text{F}$ -fluorodeoxyglucose positron emission tomography/computed tomography

to cardiovascular events may indicate a diagnosis of VaD. These two conditions can also coexist in a mixed Alzheimer's disease condition, wherein progressive memory loss exists together with features of stroke. VaD alone has a tendency to affect focal areas of primary cortical regions, cerebellum, middle temporal gyrus, and the anterior cingulate. In mixed Alzheimer's disease, common areas of involvement include the posterior parietal lobe, the posterior cingulate gyrus, prefrontal regions, and the anterior hippocampal regions.<sup>23</sup>

Figure 2 (a, b, c) shows focal areas of hypodensity noted on the CT scan (blue arrow) with the corresponding  $^{18}\text{F}$ -FDG hypometabolism in the left parietal regions and watershed areas (red arrows). A compensatory hypermetabolism was detected in the contralateral right parietal region (white arrow). Concurrent hypermetabolism was also observed in the medial temporal lobes consistent with a mixed Alzheimer's disease pattern. This type of mixed

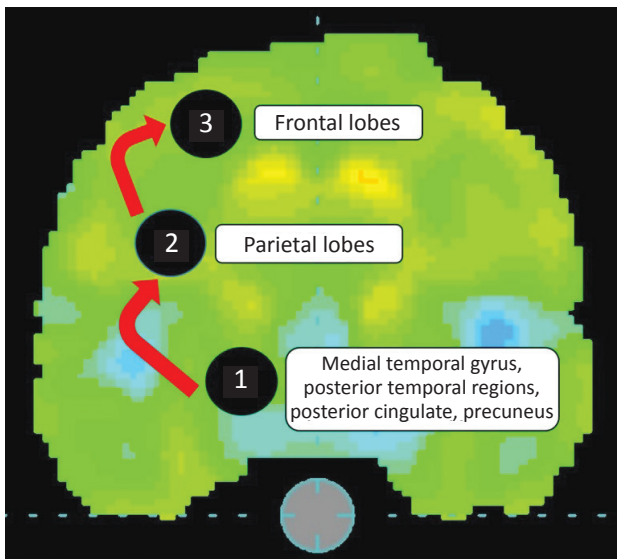


**Figure 3.** Progression of hypometabolism in Alzheimer's disease. Areas of  $^{18}\text{F}$ -fluorodeoxyglucose hypometabolism starts at the basal isocortex (1) and progressively extends into the superior and anterior regions of the cortex (2,3).

pattern has been observed in patients with mixed vascular and Alzheimer's disease, wherein areas of temporoparietal hypometabolism coexist with focal cortical areas of morphological ischemia or infarction and the corresponding  $^{18}\text{F}$ -FDG hypometabolism.<sup>24</sup>

The noncognitive behavioral changes observed in subjects with Alzheimer's disease have an implication on the metabolism in various segments of the brain. In particular, there was a significant reduction in metabolism in the frontal lobes in subjects with depressive symptoms. Among subjects with anxiety, areas of significant hypometabolism were detected at the mesial temporal lobes. As depicted in Figure 2 (d, e, f), there was a predominance of hypometabolism at the prefrontal and frontal lobes (red arrows) coexisting with the Alzheimer's disease pattern of metabolism. This finding was consistent with a history of depressive symptoms in these subjects consistent with the noncognitive behavioral changes in patients with Alzheimer's disease. In addition, patients with significant anxiety exhibited increased  $^{18}\text{F}$ -FDG metabolism in the occipital lobes and the amygdala. These findings correlated with increased eyeball activity in the overanxious subjects, which stimulated the metabolism of FDG in the visual cortex. The hypermetabolism observed in the amygdala is probably due to the emotional agitation that these anxious subjects experienced during the scan. In particular, this study demonstrated that subjects with a shorter

duration of Alzheimer's disease had a predominantly reduced activity in the medial temporal lobe, whereas subjects with advanced Alzheimer's disease exhibited a progression to the parietal and frontal lobes that resulted in global cortical hypometabolism (Figure 3).

## DISCUSSION

A clinical diagnosis of Alzheimer's disease can be made using the DSM-5 criteria in the presence of specific signs and symptoms.<sup>1</sup> However, in reality, in routine clinical settings, patients have variable presentations that can sometimes mislead the clinicians and make the diagnosis elusive. Atypical features include progressive aphasia, particularly logopenic progressive aphasia (aphasia in naming objects and repetition of sentences), and visuoperceptual or spatial syndromes, as well as emotional features, particularly apathy and anxiety.<sup>25,26</sup> In fact, other NCDs such as VaD may also be present in many of the subjects, particularly in Asian population where noncommunicable diseases related to cardiovascular disease are on the rise.<sup>27</sup> Detecting and interpreting the pathophysiological changes in a precise manner may help the clinicians to accurately treat and monitor these patients. In the past two decades, PET/CT imaging has been gaining recognition as a noninvasive biomarker for diagnosis, severity assessment, and treatment monitoring of Alzheimer's disease. Numerous studies have demonstrated that  $^{18}\text{F}$ -FDG PET/CT has a sensitivity of 60–90%<sup>28,29</sup> and a specificity of 58–73% for detecting Alzheimer's disease.<sup>28</sup> In this study, although it was detected that patients with MoCA scores  $\leq 12$  had advanced Alzheimer's disease and progressed further in their disease course, the severity of Alzheimer's disease did not significantly correlate with the observation of more than one region of hypometabolism on the  $^{18}\text{F}$ -FDG scans, i.e., the scan findings showed no correlation with the severity of the disease, which may be due to the relatively small sample size of this study.

PET/CT can be used for visual assessment and also for voxel-wise quantitative assessment. Historically, as investigated by Braak and Braak,<sup>30</sup> the progression of Alzheimer's disease was from the basal isocortex, and it can be succinctly depicted *in vivo* using  $^{18}\text{F}$ -FDG PET/CT. An interesting point to note is that despite the global hypometabolism in the cortices, the majority of patients demonstrated preserved or even hypermetabolism in the primary somatosensory cortex, S1. This finding has

**Table 3.** Clinical presentations of subjects with Alzheimer's disease correlated with 18F-FDG PET/CT findings

No.	MoCA	Clinical symptoms	PET/CT findings	Remarks
1	15	Progressive memory loss, hallucinations	↓ metabolism in one brain region (temporal lobes)	Alzheimer's disease
2	7	Memory impairment, depression, no psychotic features	↓ metabolism in ≥2 brain regions (temporoparietal and frontal lobes)	Advanced Alzheimer's disease with behavioral & mood changes
3	12	Progressive memory loss, no mood or behavioral changes	↓ metabolism in ≥2 brain regions (Global cortical hypometabolism)	Advanced Alzheimer's disease
4	8	History of left temporal stroke, progressive memory loss, hallucinations	↓ metabolism in ≥2 brain regions (Global cortical hypometabolism), ↑ metabolism in the contralateral to stroke area, ↑ metabolism S1	Advanced Alzheimer's disease with vascular Alzheimer's disease
5	8	Memory impairment, inappropriate behavior (talking to self), hallucinations, anxiety	↓ metabolism in ≥2 brain regions (Global cortical hypometabolism)	Advanced Alzheimer's disease
6	0	Memory impairment, inappropriate behavior, paranoid and impulsive	↓ metabolism in ≥2 brain regions (Global cortical hypometabolism), ↑ metabolism S1	Advanced Alzheimer's disease
7	8	Memory impairment, inappropriate behavior (talking to self), paranoid delusions, anxiety	↓ metabolism in ≥2 brain regions (Global cortical hypometabolism), ↑ metabolism S1	Advanced Alzheimer's disease with behavioral & mood changes
8	16	Progressive memory loss, anxiety	↓ metabolism in one brain region (temporal lobes) ↑ metabolism S1	Alzheimer's disease
9	20	Progressive memory loss, depression	↓ metabolism in ≥2 brain regions (temporal lobes and frontal lobes) ↑ metabolism S1	Alzheimer's disease with behavioral & mood changes
10	12	Progressive memory loss	↓ metabolism in 2 brain regions (Global cortical hypometabolism), ↑ metabolism S1	Alzheimer's disease advanced Alzheimer's disease

18F-FDG PET/CT=18F-fluorodeoxyglucose positron emission tomography/computed tomography; MoCA=Montreal cognitive assessment; ↓=reduced; ↑=increased; S1=primary somatosensory cortex

also been observed in previous studies that described that the S1 has some primitive functions that are retained even in patients with late-stage Alzheimer's disease.<sup>31</sup> This is best explained by the fact that sensory functions, which are more primitive, are preserved for a longer time despite the decline in higher cognitive abilities in patients with Alzheimer's disease.<sup>32</sup>

Voxel-wise quantification provides improved accuracy in the assessment of Alzheimer's disease, which focuses on ROIs involving multiple contiguous lobes of the brain. This method allows for a more objective assessment of the extent of cortical involvement due to the automated segmentation

provided by the computer-aided diagnosis. Clinicians can refer to the mean  $SUV_{max}$  and the SD values and compare them to a standard atlas template, thereby enabling an accurate interpretation of even subtle changes.

One of the most typical AD-related changes detected in brain images of 18F-FDG PET/CT scans includes the observation of hypometabolism in the medial/mesial temporal lobes.<sup>33</sup> In addition, subjects with noncognitive mood and behavioral changes may exhibit a predominance of hypometabolism in the frontal lobe.<sup>23</sup> Therefore, when a patient presents with noncognitive behavioral changes,

predominantly depressive symptoms, clinicians must scrutinize the frontal lobe activity to correlate the symptoms with 18F-FDG hypometabolism. Conversely, observation of frontal lobe hypometabolism may spur the clinicians to further dwell into the history of the patient's mood affects, thereby helping to tailor their medications accordingly.

Another important feature to note is the presence of morphological changes of ischemia/infarction in multiple areas of the brain, which may lead to a significant component of mixed Alzheimer's disease. These areas are likely to correspond to glucose hypometabolism and contralateral areas of compensatory hypermetabolism. This type of pattern may denote a poorer prognosis in subjects due to the gliosis that has already occurred in affected areas of the brain and is thus not amenable to pharmacological treatment.<sup>34</sup>

In a nutshell, the progression of Alzheimer's disease can be observed using the pattern of 18F-FDG hypometabolism that begins at the basal isocortex, namely, the medial temporal lobes and the hippocampus. This course then progresses to involve the parietal and frontal regions in more advanced cases. Recognition of this pattern helps in determining the advanced state of Alzheimer's disease and can serve as a biomarker for predicting the future progression of subjects with mild cognitive impairment to Alzheimer's disease. It is important to note that there is still much heterogeneity in the clinical presentation and the actual extent of glucose hypometabolism that occur in the brain, as evidenced in Table 3. This is probably due to the condition wherein altered glucose metabolism becomes more widespread in advanced NCD, causing the classical topography of several disorders to merge as a consequence of the complex neuronal interconnectivity of several regions in the brain.<sup>35</sup> Therefore, it has been proposed that such atypical or advanced cases may need to be interpreted in tandem with other parameters such as cerebrospinal fluid amyloid levels and amyloid PET/CT imaging.<sup>10</sup>

A limitation of this study was the small sample size. Therefore, it is proposed for multicenter studies with larger sample sizes to elaborate on the pattern of 18F-FDG metabolism, particularly in subjects with atypical clinical presentations and noncognitive behavioral changes. Future investigations that are

recommended include analyzing subjects with other types of NCDs to determine the pattern of metabolism in the aspect of noncognitive behavioral changes. In addition, automated segmentation of brain 18F-FDG metabolism can be performed to create computer-aided diagnosis software that can aid in the diagnosis of atypical presentation of Alzheimer's disease.

In conclusion, molecular imaging using 18F-FDG PET/CT can be applied as a noninvasive biomarker that indirectly depicts *in vivo* brain glucose metabolism, which can aid in the diagnosis of Alzheimer's disease and help in the quantification for treatment monitoring and prognostication. We recommend voxel-wise analysis and segmented quantification of 18F-FDG PET/CT images of the brain in this simplified manner, which can be clinically used by geriatricians and psychiatrists in a multidisciplinary setting for a better management of Alzheimer's disease.

#### Conflict of Interest

The authors affirm no conflict of interest in this study.

#### Acknowledgment

We would like to acknowledge the Department of Psychiatry and the memory clinic staff in Hospital Serdang, Malaysia, and Hospital Kajang, Malaysia. We also thank the Centre for Diagnostic Nuclear Imaging, Universiti Putra Malaysia, for providing excellent PET/CT images for this research.

#### Funding Sources

This study was funded by Universiti Putra Malaysia research grant, *Geran Penyelidikan Individu Berprestasi Tinggi-PUTRA*, GP-IBP/2017/9409900.

## REFERENCES

1. American Psychiatric Association. Diagnostic and statistical manual of mental disorders. Washington, D.C: American Psychiatric Association; 2013.
2. Rizzi L, Rosset I, Roriz-Cruz M. Global epidemiology of dementia: Alzheimer's and vascular types. *BioMed Res Int*. 2014;2014:908915.
3. Lestari S, Mistivani I, Rumende CM, Kusumaningsih W. Comparison between mini mental state examination (MMSE) and Montreal cognitive assessment Indonesian version (MoCA-Inda) as an early detection of cognitive impairments in post-stroke patients. *J Phys Conf Ser*. 2017;884:012153.
4. Nasreddine ZS, Phillips NA, Bédirian V, Charbonneau S, Whitehead V, Collin I, et al. The Montreal Cognitive Assessment, MoCA: a brief screening tool for mild cognitive impairment. *J Am Geriatr Soc*. 2005;53(4):695–9.
5. Martin Prince, Adelina Comas-Herrera, Martin Knapp, Maëllenn Guerchet, Karagiannidou M. World Alzheimer Report 2016: Improving healthcare for people living with dementia (Coverage, Quality and costs now and in the future). London: Alzheimer's Disease International, 2016.
6. McKhann GM, Knopman DS, Chertkow H, Hyman BT, Jack CR Jr, Kawas CH, et al. The diagnosis of dementia due to Alzheimer's disease: recommendations from the National Institute on Aging-Alzheimer's Association workgroups on diagnostic guidelines

- for Alzheimer's disease. *Alzheimers Dement*. 2011;7(3):263–9.
7. Berti V, Osorio RS, Mosconi L, Li Y, De Santi S, de Leon MJ. Early detection of Alzheimer's disease with PET imaging. *Neurodegener Dis*. 2010;7(1–3):131–5.
  8. Suppiah S, Ahmad Saad FF, Mohad Azmi NH, Nordin AJ. Mapping 18F-fluorodeoxyglucose metabolism using PET/CT for the assessment of treatment response in non-small cell lung cancer patients undergoing epidermal growth factor receptor inhibitor treatment: a single-centre experience. *Mal J Med Health Sci*. 2017;13(1):9–15.
  9. Berti V, Mosconi L, Pupi A. Brain: normal variations and benign findings in FDG-PET/CT imaging. *PET Clin*. 2014;9(2):129–40.
  10. Suppiah S, Ching SM, Nordin AJ, Vinjamuri S. The role of PET/CT amyloid imaging compared with Tc99m-HMPAO SPECT imaging for diagnosing Alzheimer's disease. *Medical J Malaysia*. 2018;73(3):141–6.
  11. Suppiah S, Chang WL, Hassan HA, Kaewput C, Asri AA, Saad FF, et al. Systematic review on the accuracy of positron emission tomography/computed tomography and positron emission tomography/magnetic resonance imaging in the management of ovarian cancer: is functional information really needed? *World J Nucl Med*. 2017;16(3):176–85.
  12. Suppiah S, Zakaria MH, Khalid B, Mohamad Saini S, Othman N. Diagnostic dilemma of reactive arthritis aided by multimodality imaging using MRI, CECT and 18F-FDG PET/CT scans. *Mal J Med Health Sci*. 2017;13(1):73–7.
  13. Erlandsson K, Buvat I, Pretorius PH, Thomas BA, Hutton BF. A review of partial volume correction techniques for emission tomography and their applications in neurology, cardiology and oncology. *Physics Med Biol*. 2012;57(21):R119–59.
  14. Smailagic N, Vacante M, Hyde C, Martin S, Ukoumunne O, Sachpekidis C. <sup>18</sup>F-FDG PET for the early diagnosis of Alzheimer's disease dementia and other dementias in people with mild cognitive impairment (MCI). *Cochrane Database Syst Rev*. 2015;1:CD010632.
  15. Minoshima S. Imaging Alzheimer's disease: clinical applications. *Neuroimaging Clin N Am*. 2003;13(4):769–80.
  16. Azmi NH, Suppiah S, Liong CW, Noor NM, Md Said S, Hanafi M, et al. Reliability of standardized uptake value normalized to lean body mass using the liver as a reference organ, in contrast-enhanced 18F-FDG PET/CT imaging. *Radiat Phys Chem*. 2018;147:35–9.
  17. Förster S, Grimmer T, Miederer I, Henriksen G, Yousefi BH, Graner P, et al. Regional expansion of hypometabolism in Alzheimer's disease follows amyloid deposition with temporal delay. *Biol Psychiatry*. 2012;71(9):792–7.
  18. Weyts K, Vernooij M, Steketee R, Valkema R, Smits M. Qualitative agreement and diagnostic performance of arterial spin labelling MRI and FDG PET-CT in suspected early-stage dementia: comparison of arterial spin labelling MRI and FDG PET-CT in suspected dementia. *Clin Imaging*. 2017;45:1–7.
  19. Zhou M, Zhang F, Zhao L, Qian J, Dong C. Entorhinal cortex: a good biomarker of mild cognitive impairment and mild Alzheimer's disease. *Rev Neurosci*. 2016;27(2):185–95.
  20. Reiman EM, Alzheimer's Disease Biomarkers Working Group for the Alliance for Aging Research. Fluorodeoxyglucose positron emission tomography: emerging roles in the evaluation of putative Alzheimer's disease-modifying treatments. *Neurobiol Aging*. 2011;32(Suppl 1):S44–7.
  21. Abdul Aziz SA, Azmi MH, Nordin AJ, Ahmad Saad FF, Ibrahim N, Wan Adnan WA, et al. Voxel-based morphometric difference in metabolic activity of 50 to 73 years old healthy adult brain: a PET/CT study. *Int J Control Theory Appl*. 2016;9(31):37–43.
  22. Borland E, Nägga K, Nilsson PM, Minthon L, Nilsson ED, Palmqvist S. The Montreal Cognitive Assessment: normative data from a large Swedish population-based cohort. *J Alzheimers Dis*. 2017;59(3):893–901.
  23. Shivamurthy VK, Tahari AK, Marcus C, Subramaniam RM. Brain FDG PET and the diagnosis of dementia. *AJR AM J Roentgenol*. 2015;204(1):W76–85.
  24. Tripathi M, Tripathi M, Damle N, Kushwaha S, Jaimini A, D'Souza MM, et al. Differential diagnosis of neurodegenerative dementias using metabolic phenotypes on F-18 FDG PET/CT. *Neuroradiol J*. 2014;27(1):13–21.
  25. Suárez-González A, Henley SM, Walton J, Crutch SJ. Posterior cortical atrophy: an atypical variant of Alzheimer disease. *Psychiatr Clin North Am*. 2015;38(2):211–20.
  26. Galton CJ, Patterson K, Xuereb JH, Hodges JR. Atypical and typical presentations of Alzheimer's disease: a clinical, neuropsychological, neuroimaging and pathological study of 13 cases. *Brain*. 2000;123(3):484–98.
  27. Kalaria RN, Maestre GE, Arizaga R, Friedland RP, Galasko D, Hall K, et al. Alzheimer's disease and vascular dementia in developing countries: prevalence, management, and risk factors. *Lancet Neurol*. 2008;7(9):812–26.
  28. Silverman DHS. Brain 18F-FDG PET in the diagnosis of neurodegenerative dementias: comparison with perfusion SPECT and with clinical evaluations lacking nuclear imaging. *J Nucl Med*. 2004;45(4):594–607.
  29. Yu P, Dean RA, Halla SD, Qi Y, Sethuraman G, Willis BA, et al. Enriching amnesic mild cognitive impairment populations for clinical trials: optimal combination of biomarkers to predict conversion to dementia. *J Alzheimers Dis*. 2012;32(2):373–85.
  30. Braak H, Braak E. Neuropathological staging of Alzheimer-related changes. *Acta Neuropathol*. 1991;82(4):239–59.
  31. Stephen JM, Montañó R, Donahue CH, Adair JC, Knoefel J, Qualls C, et al. Somatosensory responses in normal aging, mild cognitive impairment, and Alzheimer's disease. *J Neural Transm*. 2010;117(2):217–25.
  32. Teipel SJ, Stahl R, Dietrich O, Schoenberg SO, Perneczky R, Bokde AL, et al. Multivariate network analysis of fiber tract integrity in Alzheimer's disease. *Neuroimage*. 2007;34(3):985–95.
  33. Victoroff J, Lin FV, Coburn KL, Shillcutt SD, Voon V, Ducharme S. Noncognitive behavioral changes associated with Alzheimer's disease: implications of neuroimaging findings. *J Neuropsychiatry Clin Neurosci*. 2017;30(1):14–21.
  34. Reitz C. Genetic diagnosis and prognosis of Alzheimer's disease: challenges and opportunities. *Expert Rev Mol Diagn*. 2015;15(3):339–48.
  35. Brown RK, Bohnen NI, Wong KK, Minoshima S, Frey KA. Brain PET in suspected dementia: patterns of altered FDG metabolism. *Radiographics*. 2014;34(3):684–701.